

Empirical Verification of the Fe II Oscillator Strengths in the *FUSE* Bandpass¹

J. Christopher Howk, Kenneth R. Sembach, Katherine C. Roth, & Jeffrey W. Kruk

*Department of Physics and Astronomy
The Johns Hopkins University
Baltimore, MD, 21218*

howk@pha.jhu.edu, sembach@pha.jhu.edu, kroth@pha.jhu.edu, kruk@pha.jhu.edu

ABSTRACT

We report empirical determinations of atomic oscillator strengths, or f -values, for 11 ground-state transitions of Fe II in the wavelength range $1050 \lesssim \lambda \lesssim 1150$ Å. We use ultraviolet absorption line observations of interstellar material towards stars in the Galaxy and the Magellanic Clouds taken with *Copernicus*, the Goddard High Resolution Spectrograph on-board the *Hubble Space Telescope*, and the *Far Ultraviolet Spectroscopic Explorer*. We derive absolute oscillator strengths by a combination of the apparent optical depth, component fitting, and curve-of-growth fitting techniques. Our derived oscillator strengths are generally in excellent agreement with recent theoretical calculations by Raassen & Uylings using the orthogonal operator technique. However, we identify three of the eleven transitions studied here whose f -values seem to be incompatible with these calculations, by as much as a factor of two. We suggest revisions to these f -values based upon our analysis.

Subject headings: atomic data – ISM: abundances – ISM: atoms – ultraviolet: ISM

1. Introduction

The measurement and analysis of absorption lines provides the basis for much of our understanding of the content, physical conditions, and evolution of the gas-phase interstellar medium (ISM) in galaxies. Measurements of gas-phase abundances using such techniques have allowed us to study the fundamental “cosmic” abundances of the solar neighborhood (e.g., Meyer, Jura, & Cardelli 1998; Meyer, Cardelli, & Sofia 1997) and the composition and processing of interstellar dust in the warm neutral medium (e.g., Howk, Savage, & Fabian 1999; Fitzpatrick 1997; Sembach & Savage 1996; Sofia, Cardelli, & Savage 1994) and the warm ionized medium (Howk & Savage 1999). Using absorption line measurements from the *International Ultraviolet Explorer* and the *Hubble Space Telescope*, quality abundance measurements have in a few cases been extended to the ISM of the Magellanic Clouds (Welty et al. 1999a; Roth & Blades 1995) and to the high velocity cloud system of the Galaxy (Wakker et al. 1999; Lu et al. 1998). The latter examples are potentially important as low-redshift comparisons for the abundances derived in the damped Lyman- α systems (e.g., Prochaska & Wolfe 1999; Pettini et al. 1997, 1999; Lu et al. 1996), which can be used to study the chemical evolutionary history of the universe over most of a Hubble time.

¹Based on observations made with the NASA/ESA Hubble Space Telescope, obtained from the data archive at the Space Telescope Science Institute. STScI is operated by the Association of Universities for Research in Astronomy, Inc. under the NASA contract NAS 5-26555.

The recently-launched *Far Ultraviolet Spectroscopic Explorer* (*FUSE*; see Moos et al. 2000; Sahnou et al. 2000), a dedicated spectroscopic observatory operating in the wavelength range 905 to 1187 Å, will provide a wealth of data on gas-phase abundances of abundant elements in the local universe. Of these, iron is particularly important since it is both an indicator of the overall metal-enrichment of the gas as well as a significant constituent of interstellar dust grains (Savage & Sembach 1996). *FUSE* will observe interstellar clouds towards more than 50 stars in the Magellanic Clouds (e.g., Friedman et al. 2000), and tens of objects projected against high-velocity clouds (e.g., Murphy et al. 2000; Sembach et al. 2000). *FUSE* will also provide measurements of the abundances in low-redshift intergalactic absorbers (e.g., Oegerle et al. 2000; Shull et al. 2000). *FUSE* has sufficient resolution ($\lambda/\Delta\lambda \gtrsim 15,000$) to give reliable ionic column densities in many cases, if the adopted oscillator strengths are reliable.

While most of the near-ultraviolet (NUV; $\lambda \gtrsim 1200$ Å) ground-state transitions of Fe II used to determine interstellar abundances have well-determined f -values that are tied to absolute laboratory measurements (Bergeson, Mullman, & Lawler 1994, Bergeson et al. 1996, Mullman, Sakai, & Lawler 1997), the far-ultraviolet (FUV; $\lambda \lesssim 1200$ Å) transitions of Fe II are not as well constrained. In his new compilation of atomic oscillator strengths for use in absorption line measurements, Morton (2000) adopts the theoretical calculations of Raassen & Uylings (1998; hereafter RU98) in this wavelength range. These calculations, performed using the orthogonal operator technique with experimentally-determined energy levels, provide results that agree well with the laboratory measurement of many of the NUV transitions of both Fe II and Co II (with average deviations of 10% or less; see RU98).

Even though the agreement between theory and laboratory measurements for the NUV lines is encouraging, an experimental check on the f -values of the commonly-observed Fe II transitions in the *FUSE* bandpass is desirable. In this work we have empirically determined the absolute f -values of several FUV ground-state transitions of Fe II. Our emphasis is on those transitions in the wavelength range $1100 \lesssim \lambda \lesssim 1150$ Å, which contains transitions spanning more than a factor of 30 in oscillator strength, though we also present results for a few shorter-wavelength transitions. Table 1 summarizes the results of this study, giving our final derived f -values and comparing our values with empirical and theoretical values from the literature. In general we find very good agreement between our empirically-derived oscillator strengths and the theoretical results of RU98. There are several exceptions, including the transitions at 1112.048, 1121.975, and 1127.098 Å.

We have used a multi-step approach to derive the oscillator strengths given in Table 1. First, we used observations of three nearby stars (ζ Ophiuchi, δ Orionis, and μ Columbae) taken with the Goddard High Resolution Spectrograph (GHRS) on-board the *Hubble Space Telescope* (*HST*) and literature measurements from the *Copernicus* satellite to determine the f -values of several FUV transitions using apparent optical depth (AOD; Savage & Sembach 1991), component fitting (see Howk et al. 1999), and curve-of-growth fitting methods (e.g., see Jenkins 1986). The oscillator strength measurements were placed on an absolute scale by reference to NUV transitions of Fe II whose oscillator strengths have been measured in the laboratory (Mullman et al. 1997; Bergeson et al. 1994, 1996). This analysis provided reliable f -value determinations for Fe II $\lambda\lambda 1125$, 1133, 1143, and 1144² that are in excellent agreement with the theoretical calculations of RU98. This portion of our study is presented in §2.

With these well-determined absolute f -values in hand, we then used *FUSE* observations of 15 stars and curve-of-growth fitting methods to place the 1112, 1121, 1127, and 1142 Å transitions on the same absolute oscillator strength scale. Most of the sightlines used for determining these f -values are towards stars in

²We will often refer to transitions by rounding the Morton (2000) values for their wavelengths downward. Hence, Fe II $\lambda 1144$ refers to the line at 1144.938 Å.

the Large Magellanic Cloud (LMC; 12 of 15 stars); the remaining stars are located in the Small Magellanic Cloud (SMC; 2 stars) and in the low halo of the Milky Way (1 object). We find an oscillator strength for the 1142 Å transition that agrees with the calculations of RU98, although the other three transitions examined require adjustments of 30% to 140%. This phase of the study is presented in §3.

We summarize our work and discuss its implications in §4.

2. GHRS and *Copernicus* Measurements of Fe II Oscillator Strengths at Far-Ultraviolet Wavelengths

In this section we derive the absolute oscillator strengths of several FUV Fe II transitions using archival GHRS data and literature measurements from the *Copernicus* satellite.

For this treatment we have chosen to focus on three well-observed, well-studied sightlines for which high-quality GHRS data and accurate *Copernicus* measurements exist, covering both the FUV lines with unknown f -values and the NUV lines with measured f -values. The three sightlines used here are the μ Col (Howk et al. 1999; Shull & York 1977), ζ Oph (Savage, Cardelli, & Sofia 1992; Morton 1975), and δ Ori (see Bohlin et al. 1983) sightlines.

Our reduction of the archival GHRS data is discussed in §2.1. We have used three independent techniques to derive absolute Fe II oscillator strengths with these data. These are the three methods commonly used for deriving ionic column densities and include the apparent optical depth method of Savage & Sembach (1991), which we apply to the determination of f -values using the μ Col datasets in §2.2, component fitting techniques, which are applied to the μ Col sightline in §2.3, and curve-of-growth fitting, which is applied to all three sightlines in §2.4. We summarize the results of our GHRS and *Copernicus* analysis in §2.5.

2.1. GHRS Observations and Data Reduction

We have used archival GHRS observations of μ Col (HD 38666), δ Ori (HD 36486), and ζ Oph (HD 149757) to measure equivalent widths of FUV (and some NUV) Fe II transitions along these three sightlines. Although the nominal short-wavelength limit of the GHRS is 1150 Å, given the low efficiency of the MgF₂ coatings of the *HST* optics at wavelengths shortward of 1150 Å, observations at such wavelengths are possible for sufficiently bright targets. Howk et al. (1999) have demonstrated this capability, presenting GHRS observations of Fe III λ 1122, the λ 1134 triplet of N I, and Fe II λ 1133, 1143, and 1144 towards the low-halo star μ Col.

A log of the GHRS observations used in this work is given in Table 2. For the sightlines towards μ Col and ζ Oph, details of the observations at $\lambda > 1200$ Å are given by Howk et al. (1999) and Savage et al. (1992). The GHRS data towards δ Ori are presented here for the first time.

Our reduction of the archival GHRS data follows that of Howk et al. (1999). The basic calibration makes use of the standard CALHRS routine³ using the best calibration reference files as of the end of the GHRS mission. The CALHRS processing includes conversion of raw counts to count rates and corrections for particle

³CALHRS is part of the standard Space Telescope Science Institute pipeline and the STSDAS IRAF reduction package. It is also distributed via the GHRS Instrument Definition Team for the IDL package.

radiation contamination, dark counts, known diode nonuniformities, paired pulse events and scattered light. The wavelength calibration was derived from the standard calibration tables. The absolute wavelength scale should be accurate to $\sim \pm 1$ resolution element (see Table 2).

The final data reduction was performed using software developed and tested at the University of Wisconsin-Madison. This includes the merging of individual spectra and allowing for additional refinements to the scattered light correction for echelle-mode observations. The inter-order scattered light removal in GHRS echelle-mode data discussed by Cardelli et al. (1990, 1993) is based upon extensive pre-flight and in-orbit analysis of GHRS data and is used by the CALHRS routine; the coefficients derived by these authors are appropriate for observations made through the small science aperture (SSA). The scattered light coefficients for the large science aperture (LSA) observations of μ Col used in this work are given in Table 2 of Howk et al. (1999). The first-order G140M, G160M, and G200M holographic gratings have very little scattered light, and no adjustment has been made to the zero point of spectra taken with these gratings.

In all cases the GHRS absorption line data were normalized with low-order (< 5) Legendre polynomial fits to the local stellar continuum, as discussed by Sembach & Savage (1992; see their Appendix). Figure 1 shows the continuum-normalized absorption profiles of the Fe II absorption lines towards δ Ori. The top three profiles, observed with the first-order G160M grating, have a velocity resolution of $\Delta v \sim 21 \text{ km s}^{-1}$, while the lower three lines were observed with the Ech-B echelle grating at a resolution of $\Delta v \sim 3.5 \text{ km s}^{-1}$.

We have measured the equivalent widths for interstellar Fe II absorption lines along these three sightlines following Sembach & Savage (1992); these are given in Table 3. The error estimates include continuum placement uncertainties and the effects of a 2% zero-level uncertainty. Also given are *Copernicus* and GHRS literature measurements for several transitions.

The NUV ($\lambda > 1200 \text{ \AA}$) lines listed in Table 3 are considered reference transitions in our analysis. For these lines, we adopt oscillator strengths derived from the quality laboratory measurements of Mullman et al. (1997) and Bergeson et al. (1994, 1996). The laboratory determinations of the f -values for these transitions are given in Table 4 along with the f -values calculated by RU98 for comparison.

2.2. Apparent Optical Depth Analysis

The apparent optical depth method for interpreting absorption line spectra has been discussed by Savage & Sembach (1991) and Jenkins (1996). Its application to empirically deriving atomic oscillator strengths from astrophysical data has been discussed by Cardelli & Savage (1995) and Sofia, Fabian, & Howk (2000). The apparent optical depth, $\tau_a(v)$, an instrumentally-blurred version of the true optical depth of an absorption line, is given by

$$\tau_a(v) = -\ln[I(v)/I_o(v)] \quad (1)$$

where $I_o(v)$ is the estimated continuum intensity and $I(v)$ is the observed intensity of the line as a function of velocity. This is related to the apparent column density per unit velocity, $N_a(v)$ [in units $\text{atoms cm}^{-2} (\text{km s}^{-1})^{-1}$], by

$$N_a(v) = \frac{m_e c}{\pi e^2} \frac{\tau_a(v)}{f \lambda} = 3.768 \times 10^{14} \frac{\tau_a(v)}{f \lambda(\text{\AA})}, \quad (2)$$

where λ is the wavelength in \AA , and f is the atomic oscillator strength. In the absence of *unresolved* saturated structure the $N_a(v)$ profile of a line is a valid, instrumentally-blurred representation of the true column density distribution as a function of velocity, $N(v)$. Where unresolved saturated structure is present, the values of the $N_a(v)$ profile are lower limits to the true instrumentally-blurred values of $N(v)$.

For regions of absorption that are well-resolved, i.e., where $N_a(v)$ represents $N(v)$ well,

$$\tau_a(v) \propto \lambda f N(v). \quad (3)$$

If one compares two absorption lines from the same species, the ratio of their apparent optical depths over this well-resolved region should simply be the ratio of their respective values of λf . Hence, the apparent column density profiles of multiple Fe II transitions can be used to derive relative oscillator strengths.

The sightline towards μ Col exhibits a blend of warm components centered on $v_{\text{LSR}} \approx +3$ km s⁻¹ (component 1 of Howk et al. 1999) stretching from $v_{\text{LSR}} \approx -17$ to $+16$ km s⁻¹. This blend of components is well-resolved with the echelle-mode gratings of the GHRS. Howk et al. (1999) have shown lines of Fe II as strong as $\lambda 2374.461$ ($f = 0.0313$) and $\lambda 2586.650$ ($f = 0.0691$) exhibit no unresolved saturation over this velocity range (see their Figure 9). Components 2 through 4 ($v_{\text{LSR}} \approx +16$ to $+47$) along this sightline show varying degrees of unresolved saturated structure in the strongest lines.

We have used the $N_a(v)$ profiles of Fe II $\lambda\lambda 1143$ and 1144 derived from GHRS echelle-mode observations of the μ Col sightline to determine the f -values of these transitions by comparison with the $N_a(v)$ profiles of several NUV lines of Fe II. We have limited our use of the $N_a(v)$ profiles for determining f -values to those FUV transitions that were observed with the echelle-mode gratings on the GHRS with high signal-to-noise. This restriction is adopted to avoid problems with unresolved saturated structure. This limits our use of the $N_a(v)$ method of deriving oscillator strengths to the observations of Fe II $\lambda\lambda 1143$ and 1144 towards μ Col.

Using the NUV Fe II 2249.877, 2374.461, and 1608.451 Å profiles as reference transitions, we have calculated the value f_λ/f_{ref} that minimizes χ^2 for each pair of unknown (FUV) and reference (NUV) line profiles. We have used only absorption from component 1 ($v_{\text{LSR}} \approx -17$ to $+16$ km s⁻¹) to avoid potential unresolved saturated structure. The presence of such structure in the strong $\lambda 1144$ transition would reveal itself through a divergence of the $N_a(v)$ profiles for highest $\tau_a(v)$ of the strong line compared with a weaker transition. We find no evidence for such saturation in the $\lambda 1144$ profile compared with, e.g., the $\lambda 1608$ profile. However, the noise in the $\lambda 1144$ profile can cause points with high $\tau_a(v)$ to have artificially high optical depths. To avoid biases associated with low signal to noise over a limited velocity range, we have restricted our analysis to data points having $\tau_a \leq 2.5$ in determining the f -values using the $\lambda 1144$ profile.

Table 5 summarizes all of our GHRS f -value determinations, giving the RU98 theoretical f -value, the average of our determinations for each line, the individual f -value measurements, and the star, instrument, and method used in deriving those measurements. The oscillator strengths derived as described above are marked AOD (apparent optical depth) in Table 5 and represent the average value of the f -values derived using each of the three reference transitions. For $\lambda\lambda 1143$ and 1144 we derive $f = 0.0206(8)$ and $0.107(4)$, respectively, using the apparent optical depth method. The errors include contributions from the uncertainties in the reference oscillator strengths, as well as the sources of error discussed by Howk et al. (1999).

The $N_a(v)$ profiles for the FUV Fe II lines $\lambda\lambda 1144$ and 1143 are compared with the reference transitions $\lambda\lambda 1608$ and 2374 in Figure 2 using our final f -values from Table 1. The profiles of the reference lines are plotted using open squares, while the circles show the $\lambda\lambda 1144$ and 1143 profiles. For the lines shown in Figure 2, the agreement between the $N_a(v)$ profiles is excellent across the entire velocity range.

2.3. Component Fitting Analysis

The component structure of the neutral ISM along the μ Col sightline has been studied through an analysis of nearly 50 lines of 14 species from dominant ionization states (Howk et al. 1999). We make use of

the Howk et al. component structure to determine the f -values of the FUV Fe II lines, following Fitzpatrick (1997) and Sofia et al. (2000). This method of analysis is most reliable when using high-resolution data, as the details of the component structure along a sightline can be hidden at lower resolution. Hence we do not apply this method to the FUV intermediate-resolution GHRS data for any of the sightlines, which precludes use of the δ Ori and ζ Oph sightlines for determining f -values in this way.

We use the component-fitting software originally written by E. Fitzpatrick and described by Spitzer & Fitzpatrick (1993) and Fitzpatrick & Spitzer (1997). This code has been updated to account for the post-COSTAR instrumental line spread function of GHRS observations made through the LSA (see Appendix A of Howk et al. 1999). A model for the interstellar medium along the sightline was constructed by assuming a number of “clouds,” or components, along the line of sight. Each component was defined by its column density, central velocity, and Doppler spread parameter (b -value). These three parameters were varied for each component until a minimum χ^2 value between the model, convolved by the instrumental spread function, and the original data was found. In the case of Fe II, which has many ultraviolet transitions, the component structure was tested simultaneously against all of the available absorption profiles (each of which was given an input f -value).

We have derived oscillator strengths of the FUV 1143 and 1144 Å transitions by simultaneously fitting all of the Fe II lines (see Table 3 and Howk et al. 1999) observed with the echelle-mode observations, allowing not only the parameters of the component model to vary, but also the f -values of the FUV transitions. The final derived component structure is indistinguishable from the results presented in Tables 5 and 6 of Howk et al. (1999), which is expected given that the same NUV transitions are used here to define the component structure while allowing the FUV f -values to vary in the fit. Table 5 gives the resulting f -values for $\lambda\lambda 1143$ and 1144 with $\pm 1\sigma$ error estimates. We have allowed for a 4% zero-point uncertainty in the FUV lines. This seems prudent given that the observations were made through the LSA at wavelengths for which relatively little scattered light information exists for the GHRS echelle modes.

Figure 3 shows the observed absorption profiles of several Fe II profiles from the μ Col dataset with the component model overplotted. We have assumed the best-fit f -values derived through this method when displaying the 1143 and 1144 Å model profiles, namely $f = 0.0181$ and 0.120 , respectively. The ticks above the $\lambda\lambda 1143$ and 1608 profiles show the locations of the centroids of the components in the assumed model (see Howk et al. 1999).

2.4. Curve of Growth Fitting Analysis

The ionic column densities along a sightline can be derived by fitting a curve of growth to the measured equivalent widths (Jenkins 1986; Spitzer 1978). Most often this approach assumes the absorption along a sightline can be approximated by a single Gaussian (Maxwellian) absorption model (e.g., Morton 1975). While this approximation is not always valid and can yield erroneous results, particularly when using lines of large peak optical depths (see, e.g., Jenkins 1987), it is possible to derive accurate column densities through this method (Jenkins 1986).

We use curve of growth fitting for the μ Col, ζ Oph, and δ Ori sightlines, using the equivalent widths given in Table 3, to derive oscillator strengths of the FUV Fe II f -values. To do this, we fit a single-component Maxwellian curve of growth to the NUV lines of Fe II for each star. Then, using the derived column densities and b -values, we determine the oscillator strength required to make the measured equivalent widths for each FUV line in Table 3 lie on the derived curve of growth. Recent studies have used similar curve of growth

fitting techniques to derive oscillator strengths of C I (Zsargó, Federman, & Cardelli 1997), Ni II (Zsargó & Federman 1998), and Fe II (Cardelli & Savage 1995).

The results of this fitting process are summarized in Table 5. Figure 4 shows the curve of growth fit to the measured equivalent widths for the μ Col sightline. The solid points show the NUV lines used to derive the curve of growth, while the open symbols show the FUV measurements assuming the final f -values summarized in Table 1. The derived sightline-integrated column density, $\log N(\text{Fe II}) = 14.29 \pm 0.02$, is consistent with the value adopted by Howk et al. (1999), $\log N(\text{Fe II}) = 14.31 \pm 0.01$, based upon component fitting and apparent optical depth techniques. The best fit b -value is $b = 12.9 \pm 0.2 \text{ km s}^{-1}$.

For the ζ Oph sightline we derive $\log N(\text{Fe II}) = 14.49 \pm 0.02$; Savage & Sembach (1996) derive $\log N(\text{Fe II}) = 14.51 \pm 0.02$. The best fit b -value is $b = 6.6 \pm 0.2 \text{ km s}^{-1}$, consistent with the *Copernicus* study of Morton (1975). This curve of growth is shown in Figure 5. The FUV lines are placed on this diagram using the final f -values summarized in Table 1.

Towards δ Ori our best fit curve of growth gives $\log N(\text{Fe II}) = 14.08 \pm 0.03$ and $b = 10.3 \pm 1.2 \text{ km s}^{-1}$; this fit is shown in Figure 6. We have not used the 2600 Å transition in constructing this fit given its very large optical depth (see Jenkins 1987). For comparison we derive $\log N_a(\text{Fe II}) = 14.08 \pm 0.02$ by a straight integration of the $N_a(v)$ profile of $\lambda 2260$. The peak apparent optical depth of this line is $\tau_a = 0.113 \pm 0.002$. An integration of the $\lambda 2374$ profile, which has a peak apparent optical depth of $\tau_a = 1.440 \pm 0.004$, yields $\log N_a(\text{Fe II}) = 14.02 \pm 0.01$. Although this suggests a modest degree of saturation in the $\lambda 2374$ profile (all in the component centered near $v_{\text{LSR}} \approx +10 \text{ km s}^{-1}$), this line is a factor of 15 stronger than the 2260 Å transition. Given the low optical depth of the 2260 Å absorption and the relatively weak saturation for the much stronger 2374 Å line, we believe the apparent column density derived from the $\lambda 2260$ profile is an accurate measure of the true column density, which is in agreement with that derived from our curve of growth fit.

2.5. Summary of GHRS/*Copernicus* Oscillator Strength Determinations

Table 5 summarizes the results of our f -value determinations using GHRS and *Copernicus* measurements. For each transition studied, this table gives the theoretically calculated f -value from RU98 and the unweighted mean, $\langle f_\lambda \rangle$, of our individual f -value determinations. Two measures of the errors in the mean are given: the formal statistical error and, where appropriate, the standard deviation of the individual measurements, f_λ^i , about the mean. Each of the individual f -value measurements is listed, along with the sightline, instrument, and method used to derive the individual measurement.

The oscillator strengths for the transitions at 1144.938, 1143.226, 1133.665, and 1125.448 Å all not only show good agreement with the theoretical values of RU98, but also have a reasonable number of consistent individual measurements. The determination of the $\lambda 1144$ oscillator strength could potentially be prone to systematic errors in the shape of the true curves of growth of the individual sightlines. As mentioned above, it is possible that the complicated, multi-component nature of the absorption along a given line of sight could cause the true curve of growth to deviate from the theoretical single-component Maxwellian curve used in our fits (see, e.g., Morton & Bhavsar 1979). Towards δ Ori, for example, $\lambda 1144$ is the strongest transition placed on the curve of growth and is thus somewhat sensitive to the adopted b -value, which is not terribly well-constrained by the weaker transitions. Towards μ Col and ζ Oph (to a somewhat lesser extent) this transition is well-bracketed by secure measurements of the 1608.451 and 2586.650 Å lines. The agreement in the f -value derived for $\lambda 1144$ towards δ Ori with those derived for the other two sightlines is encouraging,

suggesting that the systematics in the determination are within the range of the errors. It is also encouraging to note that the apparent optical depth, component fitting, and curve of growth fitting results for μ Col are all in good agreement.

The 1055.262, 1063.972, and 1142.366 Å transitions have formally-calculated f -values that are consistent with the RU98 results. However, the individual measurements are sparse and often in poor agreement with one another. The oscillator strengths derived here for the 1121.975 and 1127.098 transitions are in poor agreement with the RU98 calculations, though there are a limited number of individual measurements for the latter line. In the next section we use *FUSE* data to constrain the oscillator strengths of several of these lines.

3. *FUSE* Measurements of Fe II Oscillator Strengths at Far Ultraviolet Wavelengths

We have derived oscillator strengths for several of the FUV Fe II transitions in the *FUSE* bandpass in the previous section. The individual determinations of the f -values of Fe II $\lambda\lambda$ 1125.448, 1133.665, 1143.226, and 1144.938 are in good agreement with one another. Furthermore, the oscillator strengths derived for these transitions are consistent with the theoretical calculations of RU98. We believe that the f -values for these FUV transitions, as given in Table 5, are secure, and we will use these oscillator strengths to derive estimates for the f -values of Fe II $\lambda\lambda$ 1112.048, 1121.975, 1127.098, and 1142.366 using a suite of *FUSE* observations of absorption along extended pathlengths through the Milky Way.

The *FUSE* data used in this section, which are summarized in Table 6, were taken in late-1999/early-2000. Most of the stars in the current sample are located in the Large Magellanic Cloud (LMC), with two objects in the Small Magellanic Cloud (SMC), and one in the Milky Way. We describe the details of the observations and reduction of the *FUSE* datasets in §3.1. The use of these *FUSE* data to constrain the remaining Fe II oscillator strengths is described in §3.2.

3.1. *FUSE* Observations and Data Reduction

The *FUSE* data for this investigation were obtained during the commissioning and early science operations stages of the *FUSE* mission. An observation log can be found in Table 6. Each observation was performed with the source centered in the $30'' \times 30''$ aperture of the LiF1 spectrograph channel.⁴ In many cases, the LiF2 channel was co-aligned well enough with the LiF1 channel that a second set of spectra covering the 1000–1187 Å wavelength range was obtained. Exposure times ranged from 3 ksec to 27 ksec for the Magellanic Cloud stars observed. The time-tagged photon event lists were processed through the standard *FUSE* calibration pipeline (*CALFUSE*) available at the Johns Hopkins University. Pipeline version 1.5.3 was used for the 1999 observations, and version 1.6.8 was used for the February 2000 observations. The photon lists were screened for valid data with constraints imposed for earth limb angle avoidance and passage through the South Atlantic Anomaly. Corrections for detector backgrounds, Doppler shifts caused by spacecraft orbital motions, and geometrical distortions were applied (Sahnow et al. 2000; see also Blair et al. 2000). No corrections were made for optical astigmatism aberrations since the data were obtained prior

⁴The K1-16 data were obtained as part of in-orbit checkout activities that required multiple exposures with the object at different locations within the aperture. The processing of this observation required special care to ensure that the individual exposures were shifted and summed properly. This will be discussed in more detail by Kruk et al. (2000, in prep.).

to completion of in-orbit focusing activities. No flatfield solutions existed at the time of these observations; therefore, we compared the LiF1 and LiF2 spectra whenever possible to determine the significance of the observed features.

The processed data have a nominal spectral resolution of 20–25 km s^{−1} (FWHM), with a relative wavelength dispersion solution accuracy of ~ 6 km s^{−1} (1σ). The zero point of the wavelength scale for each individual observation is poorly determined, although the absolute velocities of the material are not important for our purposes. When necessary, small velocity shifts were applied to individual spectral lines to ensure that the line strength comparisons were judged over a common velocity scale. In particular, the lines at 1142, 1143, and 1144 Å were systematically shifted by -20 km s^{−1} with respect to those at 1112, 1121, and 1125 Å using the dispersion solution applied to the data used in this work.

Figure 7 shows portions of the *FUSE* spectra of two O-type stars: Sk-65 22 in the LMC, and AV 232 in the SMC. These spectra represent only data from the LiF1 channel for each star. Most of the narrow interstellar lines in this bandpass are due to Fe II (see Table 1). Also present in these spectra are interstellar absorption from the Lyman (0-0) band of molecular hydrogen (near 1110.1, 1112.5, and 1115.5 Å), from Fe III at 1122.5 Å, and from a triplet of N I lines between 1134 and 1135 Å. These species are present in the Milky Way and the host galaxies of these stars, in some cases causing quite complex blending of the absorption. Prominent stellar wind lines are also visible in this spectrum, particularly the strong P Cygni profiles of P V $\lambda\lambda$ 1118.0 and 1128.0 and Si IV $\lambda\lambda$ 1122.5 and 1128.3.

We have measured equivalent widths of the Fe II lines in the spectra of all of the stars listed in Table 6 in the same manner as described above for the GHRS data. The measured equivalent widths are summarized in Table 7. For gas arising in the LMC or SMC, many of the Fe II lines with well-determined f -values are blended or in regions of uncertain continuum placement. Hence, we only present the equivalent widths of absorption lines arising from gas in the Milky Way.

The values in Table 7 are averages of the equivalent widths measured in the LiF1B and LiF2A detector segments (where the latter were available). When comparing spectra taken through the LiF1 and LiF2 channels, there are occasionally differences in the profiles of absorption lines in the two channels. This seems to be associated with the greater degree of fixed pattern noise in the LiF2A channel. Typically these profile differences result in large discrepancies in the measured equivalent widths between the two channels. In cases where the LiF1 and LiF2 measurements differ by more than 2σ , we have discarded the measurements from both channels.

3.2. Curve of Growth Fitting Analysis

Our determination of oscillator strengths using *FUSE* data relies on curve of growth fitting methods and follows the procedure discussed in §2.4. We adopt the mean f -values of Fe II $\lambda\lambda$ 1125.448, 1133.665, 1143.226, and 1144.938 from Table 1 as our reference oscillator strengths and use these to derive the f -values of $\lambda\lambda$ 1112.048, 1121.975, 1127.098, and 1142.366. The results of this fitting procedure are summarized in Table 8. This table gives the individual f -value measurements, f_{λ}^i , for each sightline. Given at the bottom of the table are the average, $\langle f_{\lambda} \rangle$, of our f -value determinations and the RU98 theoretical oscillator strengths for these transitions. The average $\lambda\lambda$ 1121, 1127, and 1142 f -values were calculated using the *FUSE* determinations and the GHRS/*Copernicus* measurements given in Table 5. Also given with the average f -values are the statistical error (in parentheses) and standard deviation of the individual measurements about the mean (in brackets).

Two sample curves of growth are shown in Figure 8. These are towards the central star of a planetary nebula, K1-16, in the Milky Way and Sk-65 22 in the LMC. Each curve of growth represents only Galactic absorption. The best-fit column densities and b -values are shown on the plots. For the sightline towards Sk-65 22, the $\lambda 1143$ absorption is not available due to blending with LMC $\lambda 1142$ absorption.

Figure 9 shows the individual f -value determinations and error estimates for the 1112.048, 1121.975, 1127.098, and 1142.366 Å transitions. The ordinate of each panel shows the derived oscillator strength of the transition. Each measurement is offset along an otherwise meaningless abscissa. The open squares in Figure 9 mark measurements made using *FUSE* data (Table 8), while the filled circles mark estimates derived from GHRS and/or *Copernicus* data (Table 5). The dotted lines show the oscillator strengths calculated by RU98, while the thick dashed lines show the unweighted means of the individual f -value determinations derived in this work.

Our measurements of the f -value for $\lambda 1142$ are consistent with the RU98 calculations. The empirically-derived oscillator strengths of the remaining three lines, however, differ significantly from the theoretical values. Of these, the 1121.975 Å transition is the most prone to systematic uncertainties in the curve of growth fitting technique. Its strength places it between the 1125 and 1144 Å transitions. It is somewhat sensitive to the adopted b -value, which is determined in large part by the strong 1144 Å transition. This could, for sightlines whose curves of growth depart strongly from the single-component, Doppler-broadened model assumed here, potentially cause systematic uncertainties in our f -value determination. Furthermore, because we only measure one line stronger than the 1121 Å transition, the determination of b -values could be skewed by systematics in the measurement of the strong 1144 Å line. The good agreement of the three GHRS/*Copernicus* determinations of $f_{\lambda 1121}$, which are quite secure, with the majority of the *FUSE* determinations suggests these systematics play a minor role. Systematics of this sort are likely of order $\lesssim 5\%$ given the the agreement of the *FUSE* and GHRS/*Copernicus* determinations.

The systematic uncertainties are likely small for the weaker 1112, 1127, and 1142 Å transitions, which all fall on or near the linear part of the curve of growth for the sightlines studied. In these cases the systematics associated with measurements of weak interstellar lines in *FUSE* data are more important than the peculiarities of the fitting procedures. It should be noted that we have found no systematic differences across our sample of sightlines between the equivalent widths measured in the LiF1 and LiF2 channels for the weak 1112, 1127, and 1142 Å transitions.

4. Discussion and Summary

We have presented a self-consistent set of empirically-derived f -values for the Fe II transitions in the range $1100 \lesssim \lambda \lesssim 1150$ Å, which are placed on an absolute scale by reference to the NUV laboratory measurements of Mullman et al. (1997) and Bergeson et al. (1994, 1996). The results of our work are summarized in Table 1, where we compare the empirically-derived f -values from this work with previous theoretical and empirical determinations. Our derived oscillator strengths agree with the orthogonal operator calculations of Raassen & Uylings (1998), with the exception of those at 1112.048, 1121.975, and 1127.098 Å. This is shown graphically in Figure 10, which displays the ratio of our best f -values to the theoretical f -values of RU98 versus their values. Over a factor of 30 range in oscillator strengths we find good agreement (within 1.5σ) between the RU98 strengths and those derived here for 8 of the 11 lines studied in this work.

Our f -value determinations are in good agreement, for the most part, with the empirical results of Lugger et al. (1982) and Shull, van Steenberg, & Seab (1983). The empirical determinations by van Buren

(1986) are at times in disagreement with our values. To some extent the agreement of our work with these empirical studies is expected since these studies used curve of growth fitting methods (which carry the heaviest weight in our averages) for some of the same sightlines used here.

We note that our derived f -value for $\lambda 1142$, $f_{\lambda 1142} = 0.0042(3)$, is in disagreement with that of Cardelli & Savage (1995), who derive $f_{\lambda 1142} = 0.00247(32)$ using GHRS observations of the star β^1 Scorpii. We believe our determination is more robust since it does not rely on a single measurement, although the dispersion of our measurements about the mean is relatively large for this transition. Welty et al. (1999b; their Appendix) discuss the potential discrepancies in FUV Fe II oscillator strengths, noting that the Cardelli & Savage (1995) f -value for $\lambda 1142$ might imply the need to revise the f -values of the 1143 and 1144 Å lines of the same multiplet. However, the RU98 calculations are in agreement with our empirical determinations for the FUV y^6F^o multiplet transitions out of the ground state.

As the *FUSE* mission proceeds, there may be other opportunities (and requirements) for studying the atomic oscillator strengths at far ultraviolet wavelengths. Some of the more important species for which it will be important to test the quality of the current oscillator strengths include O I, N I, and the shorter wavelength Fe II transitions. These species will be well-observed by *FUSE* and will allow researchers to study the gas-phase abundances in a variety of environments, but only if the oscillator strengths are reasonably well known.

We thank E. Fitzpatrick for sharing his component fitting software with us. This work is based on data obtained for the Guaranteed Time Team by the NASA-CNES-CSA FUSE mission operated by the Johns Hopkins University. Financial support to U. S. participants has been provided by NASA contract NAS5-32985.

REFERENCES

- Bergeson, S.D., Mullman, K.L., & Lawler, J.E. 1994, ApJ, 435, L157
- Bergeson, S.D., Mullman, K.L., Wickliffe, M.E., Lawler, J.E., Litzén, U., & Johansson, S. 1996, ApJ, 464, 1044
- Blair, W.P., et al. 2000, FUSE Observer’s Guide, Version 2.0 (<http://fuse.pha.jhu.edu/support/guide/guide.html>)
- Bohlin, R.C., Hill, J.K., Jenkins, E.B., Savage, B.D., Snow, T.P., Spitzer, L., & York, D.B. 1983, ApJS, 51, 277
- Cardelli, J.A., Ebbets, D.C., & Savage, B.D. 1990, ApJ, 365, 789
- Cardelli, J.A., Ebbets, D.C., & Savage, B.D. 1993, ApJ, 413, 401
- Cardelli, J.A., & Savage, B.D. 1995, ApJ, 452, 275
- Fitzpatrick, E.L. 1997, ApJ, 482, L199
- Fitzpatrick, E.L., & Spitzer, L. 1997, ApJ, 475, 623
- Friedman, S.D. et al. 2000, ApJ Letters, in press.
- Howk, J.C. & Savage, B.D. 1999, ApJ, 517, 746
- Howk, J.C., Savage, B.D., & Fabian, D. 1999, ApJ, 525, 253
- Jenkins, E.B. 1986, ApJ, 304, 739

- Jenkins, E.B. 1987, in *Interstellar Processes*, edited by D.J. Hollenbach & H.A. Thronson, Jr. (Dordrecht: Reidel), 533
- Jenkins, E.B. 1996, *ApJ*, 471, 292
- Kurucz, R.L. 1988, *Trans. IAU*, 28, 168
- Lu, L., Sargent, W.L.W., Barlow, T.A., Churchill, C.W., & Vogt, S. 1996, *ApJS*, 107, 475
- Lu, L., Savage, B.D., Sembach, K.R., Wakker, B.P., Sargent, W.L.W., & Oosterloo, T.A., 1998, *AJ*, 115, 162
- Lugger, D., Barker, E., York, D.G., Oegerle, W. 1982, *ApJ*, 259, 67
- Meyer, D.M., Cardelli, J.A., & Sofia, U.J. 1997, *ApJ*, 490, L103
- Meyer, D.M., Jura, M., & Cardelli, J.A. 1998, *ApJ*, 493, 222
- Moos, H.W., et al. 2000, *ApJ Letters*, in press.
- Morton, D.C. 1975, *ApJ*, 197, 85
- Morton, D.C. 2000, in preparation.
- Morton, D.C., & Bhavsar, S.P. 1979, *ApJ*, 228, 147
- Mullman, K.L., Sakai, M., & Lawler, J.E. 1997, *A&AS*, 122, 157
- Murphy, E.M., et al. 2000, *ApJ Letters*, in press.
- Oegerle, W.R. et al. 2000, *ApJ Letters*, in press.
- Pettini, M., Ellison, S.L., Steidel, C.C., & Bowen, D.V. 1999, *ApJ*, 510, 576
- Pettini, M., Smith, L.J., King, D.L., & Hunstead, R.W. 1997, *ApJ*, 486, 665
- Prochaska, J.X., & Wolfe, A.M. 1999, *ApJS*, 121, 369
- Raassen, A.J.J., & Uylings, P.H.M. 1998, *J. Phys. B*, 31, 3137 (RU98)
- Roth, K.C., & Blades, J.C. 1995, *ApJ*, 445, L95
- Sahnow, D.J et al. 2000, *ApJ Letters*, in press.
- Savage, B.D., Cardelli, J.A., & Sofia, U.J. 1992, *ApJ*, 401, 706
- Savage, B.D., & Sembach, K.R. 1991, *ApJ*, 379, 245
- Savage, B.D., & Sembach, K.R. 1996, *ARA&A*, 34, 279
- Sembach, K.R. et al. 2000, *ApJ Letters*, in press.
- Sembach, K.R., & Savage, B.D. 1992, *ApJS*, 83, 147
- Sembach, K.R., & Savage, B.D. 1996, *ApJ*, 457, 211
- Shull, J.M. et al. 2000, *ApJ Letters*, in press.
- Shull, J.M., Van Steenberg, M., & Seab, C.G. 1983, *ApJ*, 271, 408
- Shull, J.M., & York, D.G. 1977, 211, 803
- Sofia, U.J., Cardelli, J.A., & Savage, B. D. 1994, *ApJ*, 430, 650
- Sofia, U.J., Fabian, D., & Howk, J.C. 2000, *ApJ*, 531, 384
- Spitzer, L. 1978, *Physical Processes in the Interstellar Medium* (New York: John Wiley)
- Spitzer, L., & Fitzpatrick, E.L. 1993, *ApJ*, 409, 299

- van Buren, D. 1986, *ApJ*, 311, 400
- Wakker, B.P., Howk, J.C., Savage, B.D., Tufte, S.L., Reynolds, R.J., Benjamin, R., van Woerden, H., Schwarz, U.J., Peletier, R.F., & Kalberla, P.M.W. 1999, *Nature*, 402, 388
- Welty, D.E., Frisch, P.C., Sonneborn, G., & York, D.G. 1999a, *ApJ*, 512, 636
- Welty, D.E., Hobbs, L.M., Lauroesch, J.T., Morton, D.C., Spitzer, L., & York, D.G. 1999b, *ApJS*, 124, 465
- Zsargó, J., & Federman, S.R. 1998, *ApJ*, 498, 256
- Zsargó, J., Federman, S.R., & Cardelli, J.A. 1997, *ApJ*, 484, 820

Table 1. Recommended Fe II Oscillator Strengths for the *FUSE* Bandpass

λ_c ^a	Upper Term ^b	No. ^c	Instr. ^d	f_λ ^e	Literature f_λ -values ^f					
					RU98	Kurucz	Lugger et al.	van Buren	Shull et al.	
1055.262	$3d^5 4s 4p$	$^6P_{7/2}^o$	2	C	0.0075(14)	0.00615	0.0108	0.0074(10)	0.0092(9)	0.0080(12)
1063.972	$3d^5 4s 4p$	$^6D_{7/2}^o$	1	C	0.0037(18)	0.00475	0.00373	...	0.0041(6)	0.0045(9)
1096.877	$3d^6 5p$	$^6P_{7/2}^o$	3	C	0.032(4)	0.0327	0.0565	0.032(5)	0.0370(15)	0.032(5)
1112.048	$3d^6 5p$	$^6F_{11/2}^o$	12	F	0.0062(9)	0.00446	0.00826
1121.975	$3d^5 4s 4p$	$^6P_{7/2}^o$	17	CGF	0.0202(20)	0.0290	0.0189	0.0203(12)	0.0227(16)	0.020(3)
1125.448	$3d^6 5p$	$^6D_{7/2}^o$	2	CG	0.016(3)	0.0156	0.0261	...	0.0205(16)	0.011(3)
1127.098	$3d^6 5p$	$^6D_{9/2}^o$	12	CGF	0.0028(3)	0.00112	0.00228
1133.665	$3d^5 4s 4p$	$^6D_{7/2}^o$	3	CG	0.0055(8)	0.0047	0.0125	0.0048(5)	0.0074(11)	0.0060(9)
1142.366 ^g	$3d^5 4s 4p$	$y^6 F_{7/2}^o$	18	CGF	0.0042(3)	0.00401	0.00573	0.0050(5)	0.0060(7)	0.0050(15) ^h
1143.226	$3d^5 4s 4p$	$y^6 F_{9/2}^o$	5	CG	0.0177(12)	0.0192	0.0268	0.0133(7)	0.0200(18)	0.013(4)
1144.938	$3d^5 4s 4p$	$y^6 F_{11/2}^o$	5	G	0.106(10)	0.1090	0.1122	0.1050(5)	0.126(9)	0.105(21)

^aVacuum wavelengths (in Å) from Morton (2000).

^bDesignation of the upper term of the transition. All transitions arise from the ground state, $3d^6(a^5D)4s^6D_{9/2}$.

^cNumber of individual f_λ^i determinations used in deriving the final value presented in this table.

^dThe instrument(s) used in deriving each f_λ , where C, G, and F denote *Copernicus*, GHRS, and *FUSE*, respectively.

^eFinal derived oscillator strengths from the current work. The numbers in parentheses denote the uncertainties in the last digit(s).

^fSelected literature values of Fe II oscillator strengths for comparison with those derived in the current work. The columns give literature f -values from the calculations of Raassen & Uylings (1998; adopted by Morton 2000) and Kurucz (1988), and from the empirical (astrophysical) determinations by Lugger et al. (1982), van Buren (1986), and Shull et al. (1983), respectively. The numbers in parentheses denote the uncertainties in the last digit(s).

^gCardelli & Savage (1995) have also used the GHRS to empirically estimate this f -value. They derive $f_{\lambda 1142} = 0.00247(32)$ based only on the sightline towards β^1 Scorpii using a curve-of-growth fit.

^hShull et al. (1983) give a value of 0.050(15) in their Table 3. This is a typo that has been corrected for the current table (J.M. Shull, 2000, priv. comm.).

Table 2. GHRs Observation Log^a

Spectra Range [Å]	Rootname ^b	Exp. Time [sec]	Grating	Resolution ^c [km s ⁻¹]	Aper. ^d	COSTAR? ^e
μ Columbae						
1116-1124	Z2X30108T	81.6	G140M	16.	LSA	Yes
	Z2X30109T	81.6	G140M	16.	LSA	Yes
1131-1137	Z2C0011AP	108.8	Ech-A	3.5	LSA	Yes
1142-1148	Z2AF011AT	108.8	Ech-A	3.5	LSA	Yes
	Z2C0030RT	108.8	Ech-A	3.5	LSA	Yes
	Z308010OT	108.8	Ech-A	3.5	LSA	Yes
	Z3JN010OT	108.8	Ech-A	3.5	LSA	Yes
δ Orionis A						
1127-1164	Z1850107T	217.6	G160M	21.	SSA	No
2256-2265	Z185020KT	13.6	Ech-B	3.5	SSA	No
	Z185020LT	13.6	Ech-B	3.5	SSA	No
	Z185020MT	13.6	Ech-B	3.5	SSA	No
2367-2377	Z185020NT	13.6	Ech-B	3.5	SSA	No
	Z185020OT	13.6	Ech-B	3.5	SSA	No
	Z185020PT	13.6	Ech-B	3.5	SSA	No
2599-2609	Z185020QT	13.6	Ech-B	3.5	SSA	No
	Z185020RT	13.6	Ech-B	3.5	SSA	No
	Z185020ST	13.6	Ech-B	3.5	SSA	No
ζ Ophiuchi						
1126-1154	Z0HU020WM	68.0	G140M	15.	SSA	No
	Z0HU520UT	68.0	G140M	15.	SSA	No
1603-1638	Z0HU012AT	13.6	G160M	14.	LSA	No
2241-2279	Z0HU013JM	13.6	G200M	11.	LSA	No
2334-2347	Z0XZ010BT	5.6	Ech-B	3.5	SSA	No

^aThis table describes the GHRs exposures used in this work. For μ Col and ζ Oph, we list only those datasets covering $\lambda < 1200$ Å. The longer wavelength GHRs data for μ Col are described by Howk et al. (1999) and the ζ Oph data are discussed by Savage et al. (1992).

^bSTScI archival rootname.

^cApproximate velocity resolution (FWHM) in km s⁻¹.

^dThe entrance aperture used for the observation. Here SSA refers to the small science aperture (pre-COSTAR: $0''.24 \times 0''.24$; post-COSTAR: $0''.22 \times 0''.22$) and LSA refers to the large science aperture (pre-COSTAR: $2''.00 \times 2''.00$; post-COSTAR: $1''.74 \times 1''.74$)

^eDenotes observations taken before (No) or after (Yes) the installation of the Corrective Optics Space Telescope Axial Replacement (COSTAR) unit.

Table 3. GHRS/*Copernicus* Fe II Equivalent Width Measurements

λ_c^a [Å]	μ Col ^b		δ Ori ^c		ζ Oph ^d	
	W_λ [mÅ]	Instr. ^e	W_λ [mÅ]	Instr. ^e	W_λ [mÅ]	Instr. ^e
1055.262	11.2 ± 2.0	<i>Cop</i>	$21(\pm 3)$	<i>Cop</i>
1063.972	7 ± 3	<i>Cop</i>
1096.877	53 ± 3	<i>Cop</i>	30.0 ± 0.7	<i>Cop</i>	$52(\pm 3)$	<i>Cop</i>
1121.975	34 ± 4	G140M	22.4 ± 1.3	<i>Cop</i>	$42(\pm 3)$	<i>Cop</i>
1125.448	27 ± 4	G140M	$39(\pm 3)$	<i>Cop</i>
1127.098	10.5 ± 2.1	<i>Cop</i> /G140M
1133.665	14.0 ± 2.5	Ech-A	6.1 ± 0.5	<i>Cop</i>	15.5 ± 1.9	<i>Cop</i> /G140M
1142.366	4.1 ± 0.7	G160M	17.9 ± 1.9	<i>Cop</i> /G140M
1143.226	34.8 ± 1.1	Ech-A	20.2 ± 0.7	G160M	37.9 ± 2.2	<i>Cop</i> /G140M
1144.938	112.9 ± 2.1	Ech-A	74.7 ± 0.9	G160M	80.7 ± 1.4	G140M
1608.451	144.4 ± 2.4	Ech-A	103 ± 3	G160M
2249.877	14.2 ± 0.4	Ech-B	22.5 ± 1.1	Ech-B
2260.780	21.9 ± 0.6	Ech-B	12.9 ± 0.7	Ech-B	31 ± 4	G200M
2344.214	302 ± 4	Ech-B	195 ± 4	Ech-B
2374.461	182 ± 3	Ech-B	125 ± 3	Ech-B	149.2 ± 1.3	Ech-B
2586.650	291 ± 4	Ech-B
2600.173	388 ± 5	Ech-B	370 ± 7	Ech-B

^aCentral wavelengths from Morton (2000).

^bThe *Copernicus* equivalent width measurements towards μ Col are from Shull & York (1977). The GHRS measurements for $\lambda_c > 1133$ Å are from Howk et al. (1999), while the remaining GHRS G140M measurements are from this work.

^cThe δ Ori *Copernicus* measurements are from Bohlin et al. (1983) while the GHRS measurements are from this work.

^dThe ζ Oph *Copernicus* measurements are from Morton (1975). The $\lambda\lambda 2249, 2374$ Ech-B GHRS measurements are from Savage et al. (1992). The remaining GHRS measurements are from this work. Where no error measurement was quoted for the *Copernicus* equivalent widths we assumed a 1σ error of 3 mÅ. Such errors are given in parentheses. Both GHRS and *Copernicus* equivalent width measurements were available for several transitions. In most of these cases the measurements agreed to within 1σ of the GHRS measurements. Where two measurements are available, and the *Copernicus* data seem of high quality, we averaged the equivalent widths from these two instruments.

^eThe instrument with which the measurements were made. In this case *Cop* refers to measurements made with the *Copernicus* satellite, while GHRS measurements are listed according to the grating used: Ech-A, Ech-B, G140M, G160M, or G200M.

Table 4. Near Ultraviolet Fe II Oscillator Strengths

λ_c [Å] ^a	f_λ ^b	Ref. ^c	f_{RU98} ^d
1608.451	0.058(5)	1	0.054
2249.877	0.00182(14)	2	0.00218
2260.780	0.00244(19)	2	0.00262
2344.214	0.114(2)	2	0.125
2374.461	0.0313(14)	2	0.0329
2586.650	0.0691(25)	2	0.0709
2600.173	0.239(4)	2	0.242

^aCentral wavelength from Morton (2000).

^bAdopted experimental oscillator strength.

^cReference for adopted experimental oscillator strengths: (1) Mullman et al. (1997); (2) Bergeson et al. (1996).

^dTheoretical oscillator strength from Raassen & Uylings (1998) for comparison.

Table 5. Summary of GHRS/*Copernicus* Results

λ_c^a	f_{RU98}^b	$\langle f_\lambda \rangle^c$	$f_\lambda^i{}^d$	Star	Instrument ^e	Method ^f
1055.262	0.00615	0.0075(14)[-]	0.0061(16)	μ Col	<i>Cop</i>	CoG
			0.0088(22)	ζ Oph	<i>Cop</i>	CoG
			0.0037(18)	μ Col	<i>Cop</i>	CoG
1063.972	0.00475	0.0037(18)[-]	0.0037(18)	μ Col	<i>Cop</i>	CoG
1096.877	0.0327	0.032(4)[3]	0.034(7)	μ Col	<i>Cop</i>	CoG
			0.028(6)	δ Ori	<i>Cop</i>	CoG
			0.033(9)	ζ Oph	<i>Cop</i>	CoG
1121.975	0.0290	0.019(3)[1]	0.018(4)	μ Col	G140M	CoG
			0.019(4)	δ Ori	<i>Cop</i>	CoG
			0.020(5)	ζ Oph	<i>Cop</i>	CoG
1125.448	0.0156	0.016(3)[3]	0.014(4)	μ Col	G140M	CoG
			0.018(4)	ζ Oph	<i>Cop</i>	CoG
1127.098	0.00112	0.0034(9)[-]	0.0034(9)	ζ Oph	G140M/ <i>Cop</i>	CoG
1133.665	0.0047	0.0055(8)[11]	0.0067(18)	μ Col	Ech-A	CoG
			0.0046(10)	δ Ori	<i>Cop</i>	CoG
			0.0052(12)	ζ Oph	G140M/ <i>Cop</i>	CoG
1142.366	0.00401	0.0045(8)[-]	0.0031(8)	δ Ori	G160M	CoG
			0.0060(13)	ζ Oph	G140M/ <i>Cop</i>	CoG
1143.226	0.0192	0.0177(12)[18]	0.018(4)	μ Col	Ech-A	CoG
			0.0206(8)	μ Col	Ech-A	AOD
			0.0181(13)	μ Col	Ech-A	CF
			0.016(3)	δ Ori	G160M	CoG
			0.016(3)	ζ Oph	G140M/ <i>Cop</i>	CoG
1144.938	0.1090	0.106(10)[11]	0.11(3)	μ Col	Ech-A	CoG
			0.107(4)	μ Col	Ech-A	AOD
			0.120(18)	μ Col	Ech-A	CF
			0.09(3)	δ Ori	G160M	CoG
			0.104(17)	ζ Oph	G140M	CoG

^aVacuum wavelengths (in Å) from Morton (2000).

^bTheoretical values of f_λ calculated by Raassen & Uylings (1998). These oscillator strengths are adopted in the new compilation of Morton (2000).

^cAverage values of f_λ with 1σ statistical uncertainties of the last digits in parentheses. The standard deviations of the individual measurements f_λ^i about the mean are given in square brackets.

^dIndividual measurements f_λ^i of the oscillator strengths with 1σ errors in the last digit(s) given in parentheses.

^eInstrument used in deriving the individual oscillator strength estimates: *Cop* refers to data taken with the *Copernicus* satellite, while Ech-A, G140M, and G160M refer to the gratings used in GHRS observations. The *Copernicus* data for μ Col, ζ Oph, and δ Ori are taken from Shull & York (1977), Morton (1975), and Bohlin et al. (1983), respectively.

^fMethod used for deriving the individual f -value measurement, f_λ^i : CoG - curve of growth fitting; AOD - apparent optical depth/column density method; and CF - component fitting.

Table 6. *FUSE* Observation Log

Star	Altern. Name	Dataset	Date ^a	Exp. Time [ksec]	S/N ($\lambda 1125$) ^b	Notes
K1-16 ^c	...	I81103**	10/15/99	40.0	30	CSPN
AV 232	Sk 80	X0200201	09/25/99	10.3	18	SMC
HD 5980	Sk 78	X0240202	10/20/99	3.2	18	SMC
Sk-65 22	HD 270952	P1031002	12/20/99	27.2	17	LMC
Sk-67 104	HD 36402	P1031302	12/17/99	5.1	13	LMC
Sk-68 80	HD 36521	P1031402	12/17/99	9.7	17	LMC
Sk-69 246	HD 38282	P1031802	12/16/99	22.1	10	LMC
Sk-67 211	HD 269810	P1171603	12/20/99	8.2	16	LMC
Sk-67 69	...	P1171703	12/20/99	6.2	8	LMC
Sk-67 167	LH76:21	P1171902	12/17/99	2.8	11	LMC
Sk-66 100	...	P1172303	12/20/99	7.1	8	LMC
Sk-70 115	HD 270145	P1172601	02/12/00	5.2	13	LMC
BI 229	...	P1172801	02/11/00	5.6	17	LMC
Sk-67 111	LH60:53	P1173001	02/11/00	8.0	19	LMC
Sk-69 249	HD 269927	P1174601	02/09/00	7.2	23	LMC

^aDate of observation.

^bEmpirical signal to noise estimate near 1125 Å in the LiF1 channel.

^cThe K1-16 data were obtained as part of in-orbit checkout activities. Since the object was observed at several different locations within the aperture, the processing of these data required special processing to ensure that the individual exposures were shifted and summed properly. This will be discussed in more detail by Kruk et al. (2000, in prep.).

Table 7. *FUSE* Fe II Equivalent Width Measurements

Star	W_λ [mÅ] ^a							
	$\lambda 1112.048$	$\lambda 1121.975$	$\lambda 1125.448$	$\lambda 1127.098$	$\lambda 1133.665$	$\lambda 1142.366$	$\lambda 1143.226$	$\lambda 1144.938$
K1-16	33 ± 2	92 ± 3	83 ± 3	18 ± 2	32 ± 3	28 ± 3	86 ± 3	171 ± 4
AV 232	45 ± 5	65 ± 6	63 ± 4	16 ± 4	42 ± 5	24 ± 4	76 ± 6	132 ± 4
HD 5980	64 ± 5	20 ± 4	34 ± 5	25 ± 6	60 ± 5	128 ± 4
Sk-67 05 ^c	...	85 ± 2	78 ± 2	16 ± 2	38 ± 5	16 ± 3	...	173 ± 4
Sk-65 22	28 ± 5	95 ± 5	70 ± 3	17 ± 4	29 ± 5	19 ± 3	...	192 ± 4
Sk-67 104	...	85 ± 6	73 ± 4	18 ± 5	37 ± 5	28 ± 5	...	148 ± 5
Sk-68 80	41 ± 4	84 ± 5	74 ± 3	16 ± 3	25 ± 4	21 ± 3	...	151 ± 4
Sk-69 246	42 ± 7	107 ± 6	87 ± 7	18 ± 4	25 ± 4	26 ± 3	...	213 ± 6
Sk-67 211	32 ± 4	104 ± 7	71 ± 5	16 ± 4	28 ± 5	39 ± 4	...	145 ± 10
Sk-67 69	40 ± 9	83 ± 8	80 ± 7	...	31 ± 4	18 ± 5	...	172 ± 9
Sk-67 167	...	74 ± 5	64 ± 5	...	27 ± 4	23 ± 4	69 ± 4	138 ± 4
Sk-66 100	40 ± 5	73 ± 5	72 ± 5	...	41 ± 6	23 ± 5	70 ± 6	125 ± 5
Sk-70 115	56 ± 6	96 ± 6	90 ± 5	...	31 ± 6	32 ± 5	93 ± 5	...
BI 229	19 ± 4	62 ± 3	55 ± 3	13 ± 4	27 ± 5	22 ± 3	76 ± 5	160 ± 6
Sk-67 111	29 ± 3	70 ± 4	64 ± 3	...	33 ± 3	22 ± 3	73 ± 3	145 ± 3
Sk-69 249	33 ± 4	91 ± 3	71 ± 3	14 ± 3	33 ± 3	29 ± 2

^aThe equivalent width measurements and 1σ errors given here are averages of the LiF1B and LiF2A observations for these sightlines.

^bThe equivalent widths for Sk-67 05 are from Friedman et al. (2000).

Table 8. Summary of *FUSE* f -value Determinations

Star	$f_{\lambda}^{i\text{ a}}$			
	$\lambda 1112.048$	$\lambda 1121.975$	$\lambda 1127.098$	$\lambda 1142.366$
K1-16	0.0052(5)	0.0203(20)	0.0025(3)	0.0041(5)
AV 232	0.0082(15)	0.014(3)	0.0022(7)	0.0035(8)
HD 5980	0.0036(9)	0.0046(14)
Sk-67 05	...	0.0186(17)	0.0024(4)	0.0023(5)
Sk-65 22	0.0055(12)	0.025(3)	0.0031(9)	0.0035(7)
Sk-67 104	...	0.020(4)	0.0027(9)	0.0042(10)
Sk-68 80	0.008(4)	0.019(7)	0.0031(11)	0.0038(14)
Sk-69 246	0.0076(16)	...	0.0029(8)	0.0043(8)
Sk-67 211	0.0059(14)	0.035(12)	0.0026(9)	0.0070(17)
Sk-67 69	0.0072(23)	0.019(4)	...	0.0028(9)
Sk-67 167	...	0.021(3)	...	0.0043(9)
Sk-66 100	0.0066(17)	0.017(4)	...	0.0032(10)
Sk-70 115	0.010(6)	0.019(11)	...	0.005(3)
BI 229	0.0043(10)	0.0167(21)	0.0027(10)	0.0046(8)
Sk-67 111	0.0055(8)	0.0175(22)	...	0.0039(6)
Sk-69 249	0.0076(16)	...	0.0029(8)	0.0043(8)
$\langle f_{\lambda} \rangle^{\text{b}}$	0.0062(9)[16]	0.0202(20)[46]	0.0028(3)[5]	0.0042(3)[11]
$f_{\text{RU98}}^{\text{c}}$	0.00446	0.0290	0.00112	0.00401

^aIndividual measurements f_{λ}^i of the oscillator strengths with 1σ errors in the last digit(s) given in parentheses.

^bAverage value of f_{λ} with 1σ statistical uncertainties of the last digits in parentheses. The standard deviations of the individual measurements f_{λ}^i about the mean are given in square brackets.

^cTheoretical values of f_{λ} from the calculations of Raassen & Uylings (1998).

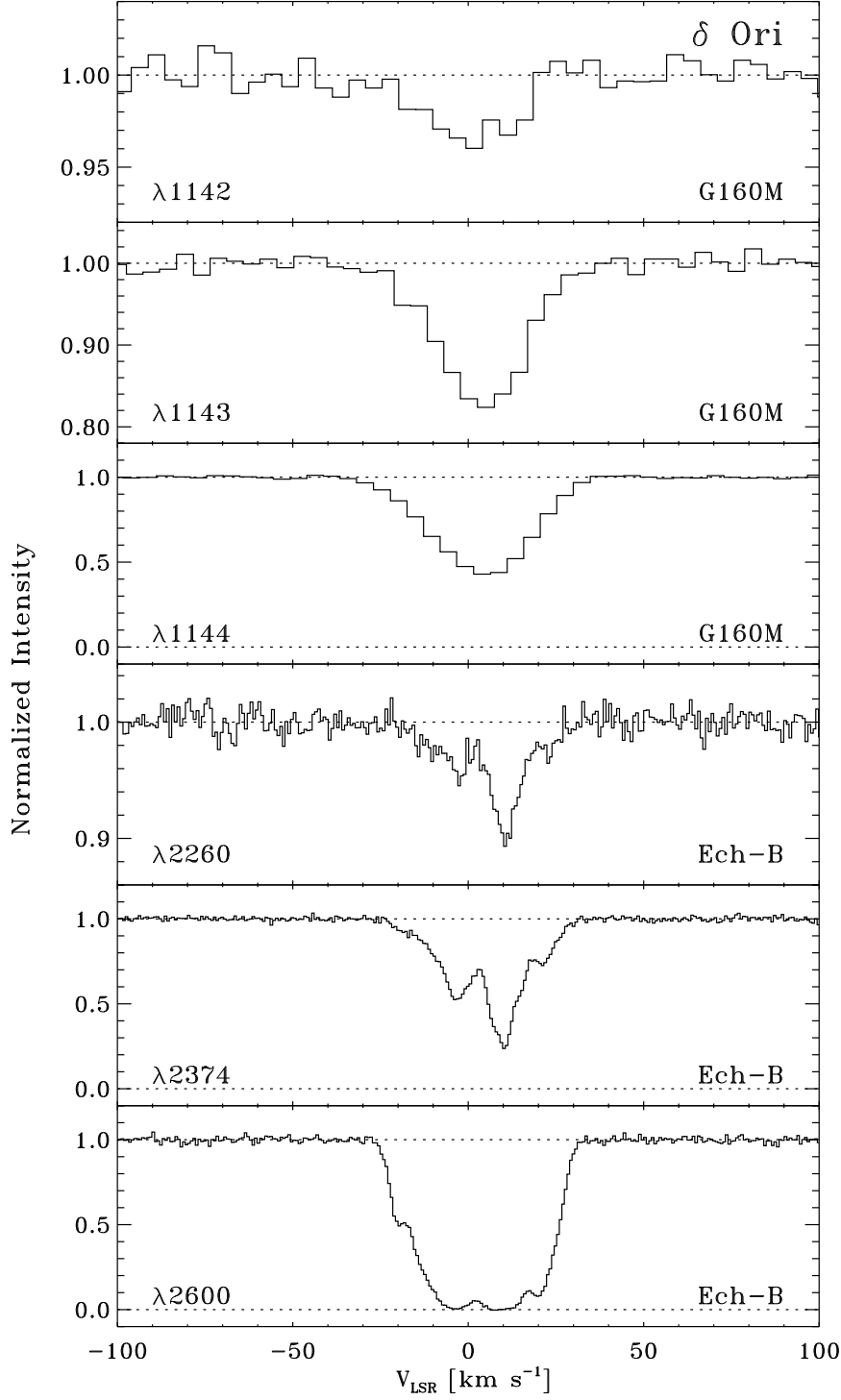


Fig. 1.— Continuum-normalized GHRs absorption line spectra of the measured Fe II transitions towards δ Orionis. The velocity scale is with respect to the local standard of rest (LSR), and no adjustments have been made to the default wavelength calibrations of the data. The Ech-B data have a resolution of $\Delta v \sim 3.5$ km s $^{-1}$; the G160M data have a resolution $\Delta v \sim 21$ km s $^{-1}$.

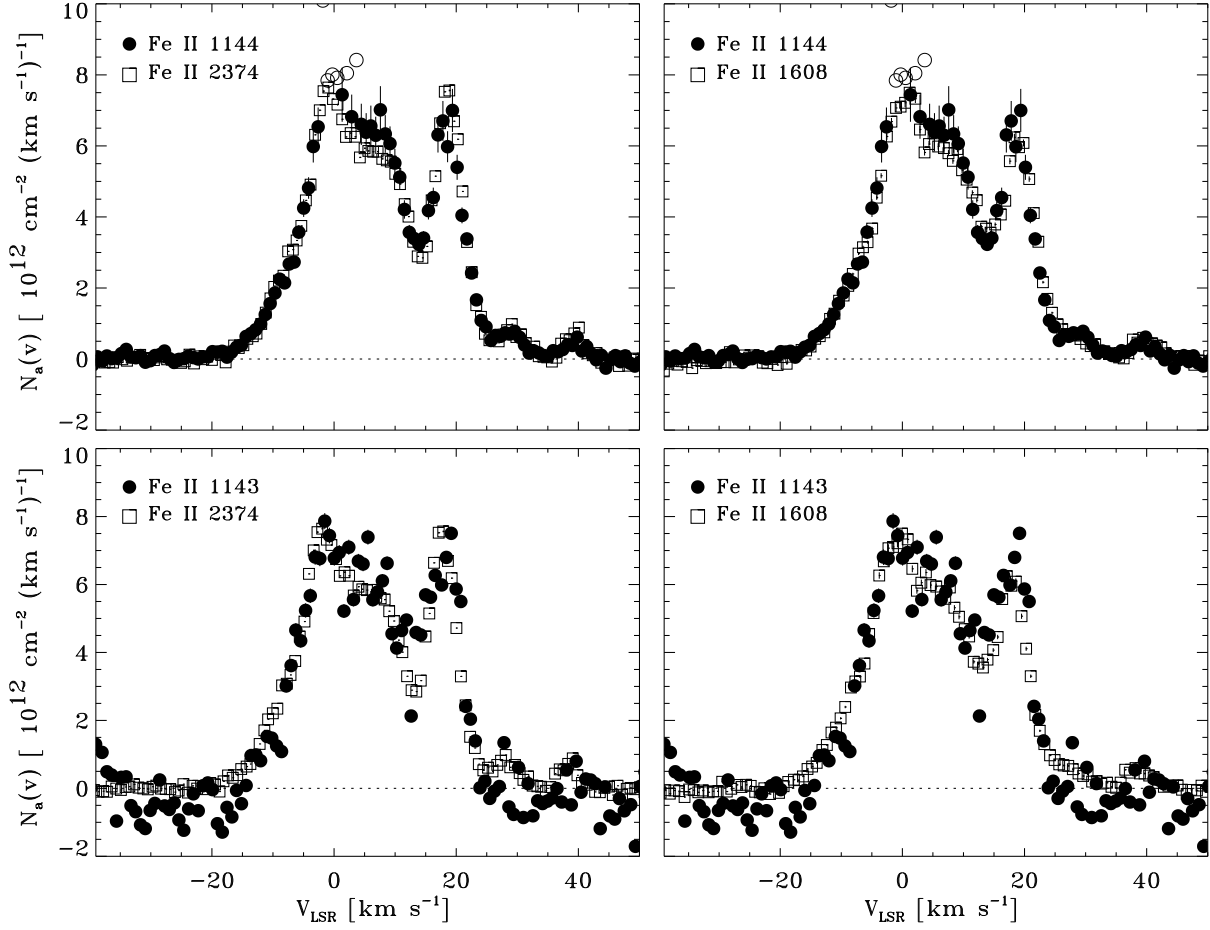


Fig. 2.— Apparent column density profiles for the FUV transitions of Fe II at 1143.226 and 1144.938 Å compared with the reference lines at 1608.451 and 2374.461 Å for the sightline to μ Col. The circles show the FUV profiles while the open squares denote the reference lines. The open circles in the plots containing the $\lambda 1144$ profile show points that were not used in determining the f -values because $\tau_a \geq 2.5$.

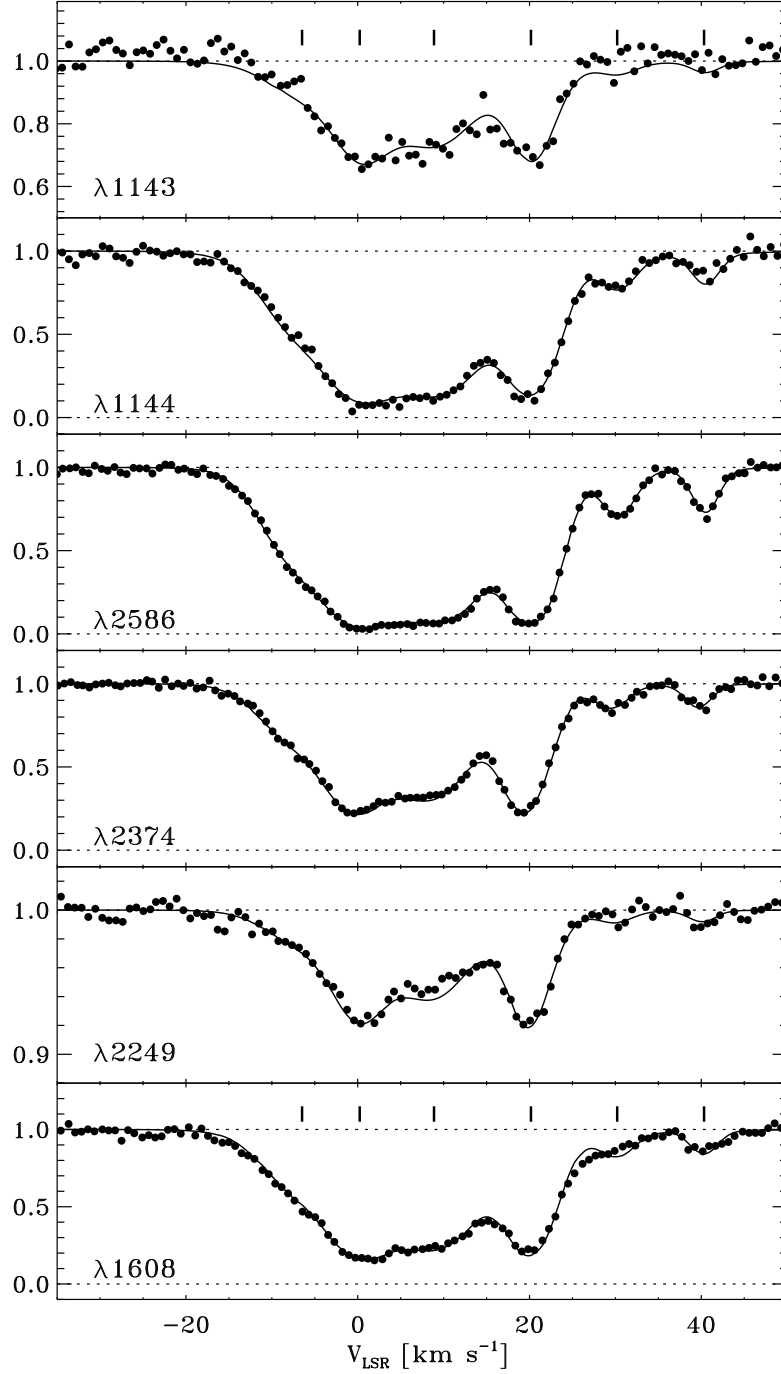


Fig. 3.— Continuum-normalized GHRs absorption line spectra of several Fe II transitions towards μ Col. The filled dots show the GHRs data, while the solid lines show the best-fit component model of the absorption along this sightline. The ticks above the $\lambda\lambda 1608$ and 1143 profiles show the locations of the velocity centroids for the adopted component model. The model profiles use the f -values from Table 4, except for the $\lambda\lambda 1143$ and 1144 models. For these lines we use the best-fit f -values determined through our component fitting analysis (see Table 1).

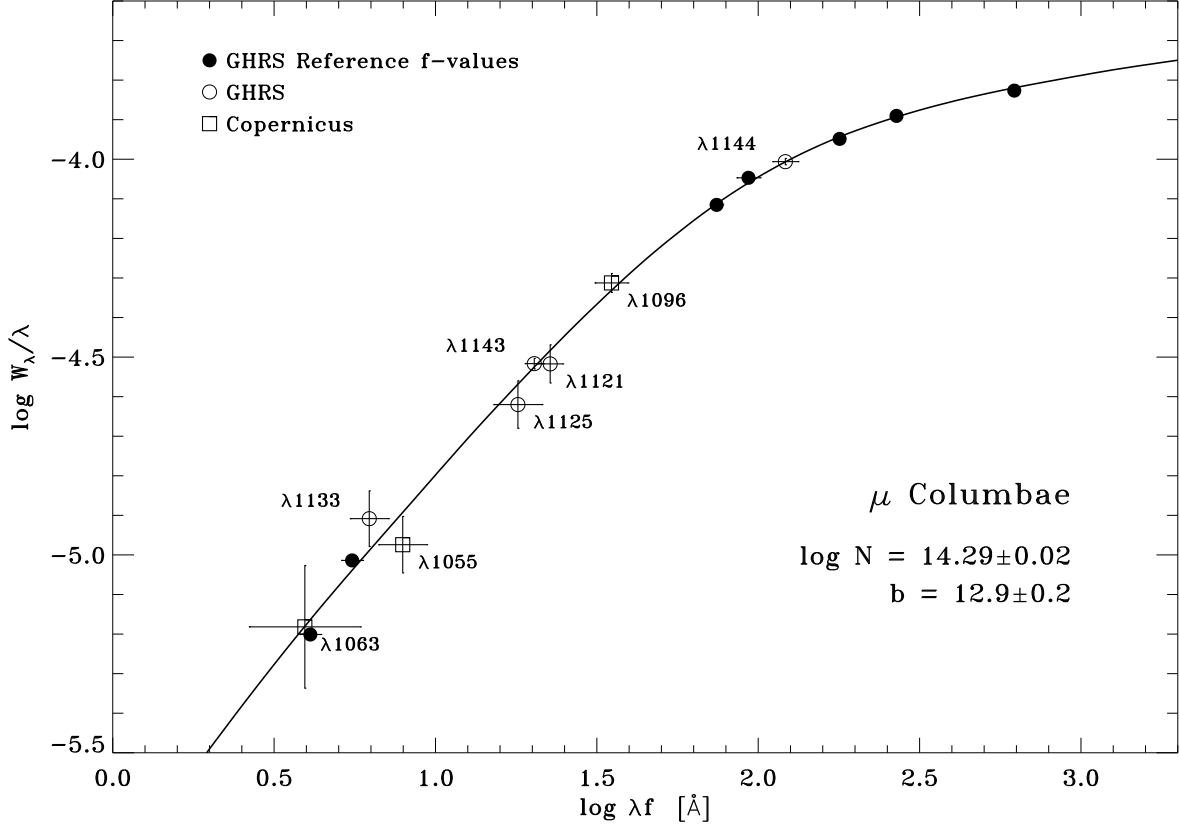


Fig. 4.— The best-fit, single-component curve of growth for the μ Col Fe II data. This curve was fit to GHRs measurements of transitions with well-determined f -values (filled circles). The GHRs measurements (open circles) and *Copernicus* measurements (open squares) of FUV transitions are placed on this diagram using our final oscillator strength estimates (see Table 1). The error bars in the equivalent width measurements for the reference transitions are typically smaller than the filled plotting symbols. The column density derived from this curve of growth, $\log N(\text{Fe II}) = 14.29 \pm 0.02$, is consistent with the value $\log N(\text{Fe II}) = 14.31 \pm 0.01$ adopted by Howk et al. (1999) for this sightline using component-fitting techniques.

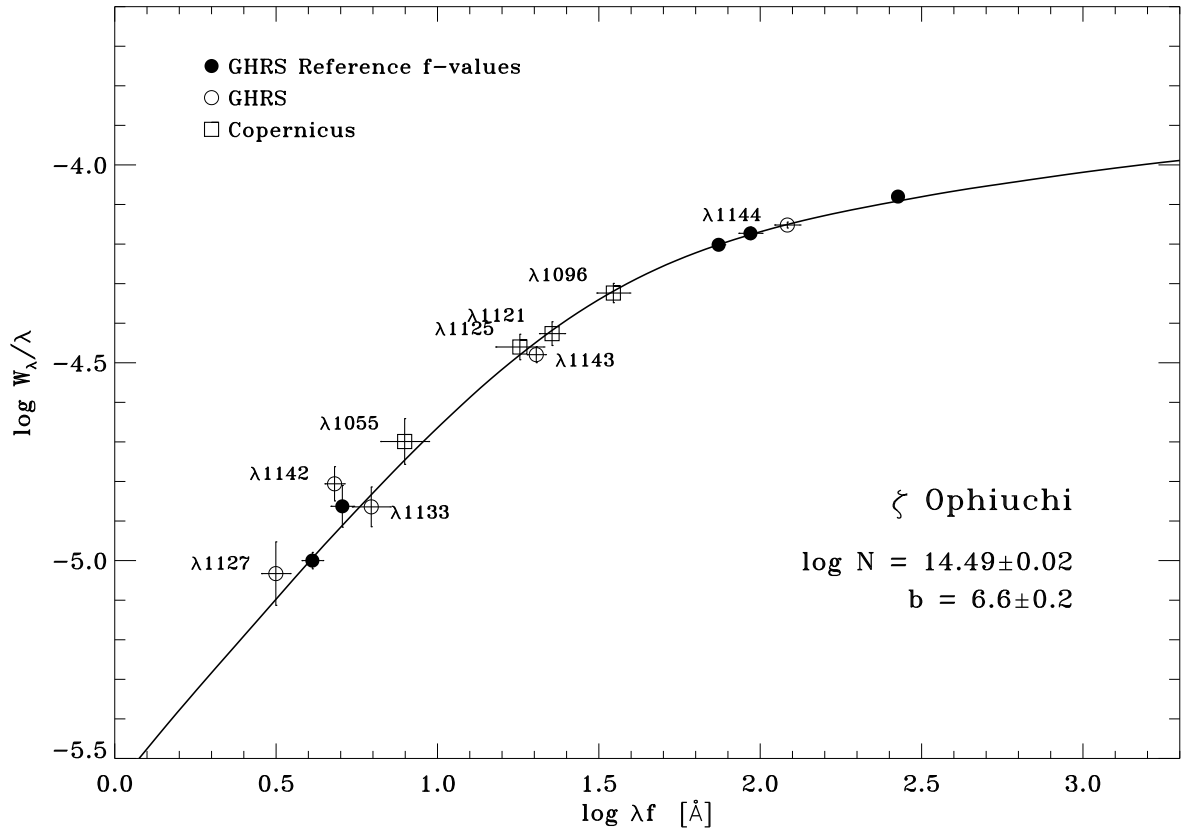


Fig. 5.— As Figure 4, but for the sightline towards ζ Oph. The best fit column density, $\log N(\text{Fe II}) = 14.49 \pm 0.02$, is consistent with the value $\log N(\text{Fe II}) = 14.51 \pm 0.02$ adopted by Savage & Sembach (1996).

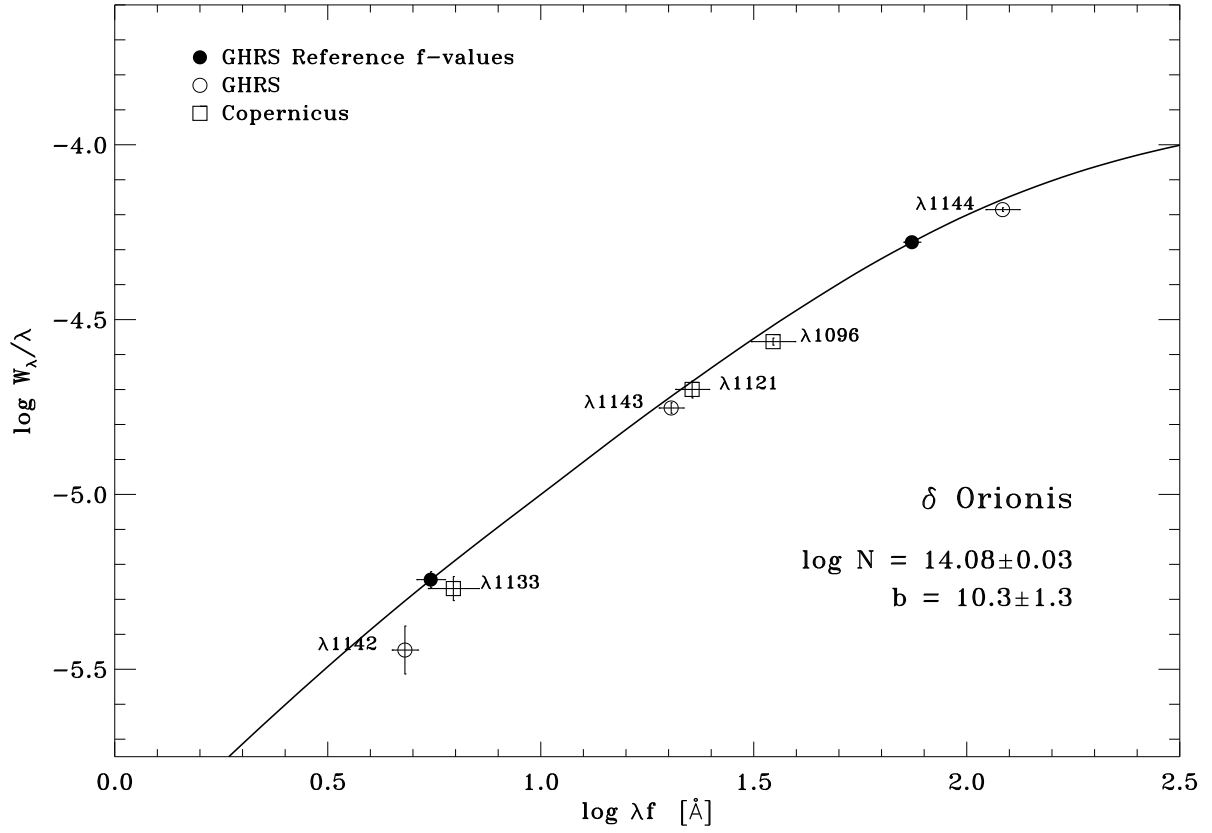


Fig. 6.— As Figure 4, but for the sightline towards δ Ori. The best fit column density is $\log N(\text{Fe II}) = 14.08 \pm 0.03$.

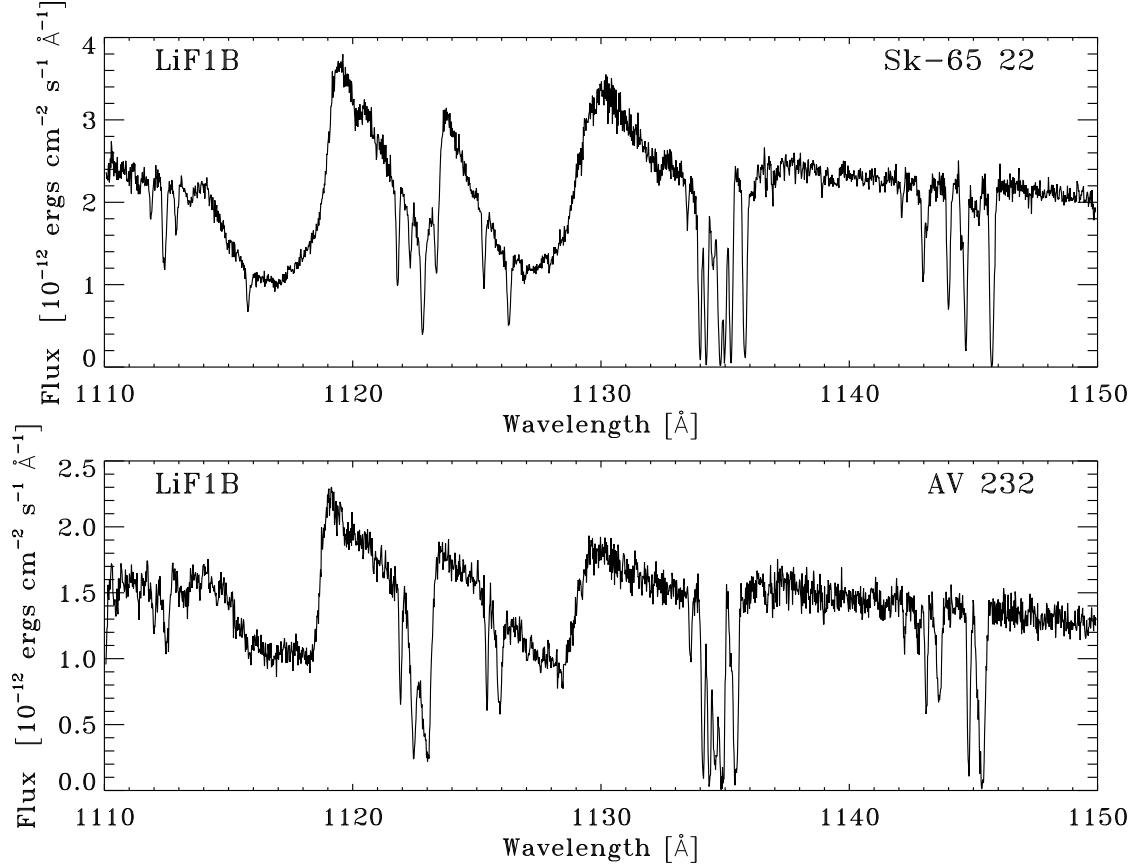


Fig. 7.— *FUSE* spectra of the O6Iaf+ star Sk-65 22 in the LMC (*top*) and the O7Iaf+ star AV 232 in the SMC (*bottom*) over the range $1100 \lesssim \lambda \lesssim 1150$ \AA . These plots show only data from the LiF1 channel, and the data have a resolution $\Delta v \gtrsim 20$ km s^{-1} . These spectra show absorption from interstellar Fe II in the Milky Way as well as both Magellanic Clouds at rest wavelengths of 1112.048, 1121.975, 1125.448, 1127.098, 1133.665, 1142.366, 1143.226, and 1144.938 \AA . Also seen are interstellar lines of molecular hydrogen near 1112 \AA , Fe III at 1122.524 \AA , and a triplet of N I lines near 1135 \AA . Several prominent P Cygni stellar wind profiles are seen in this band, including the P V doublet at 1117.977 and 1128.008 \AA and the Si IV lines at 1122.486 and 1128.339 \AA .

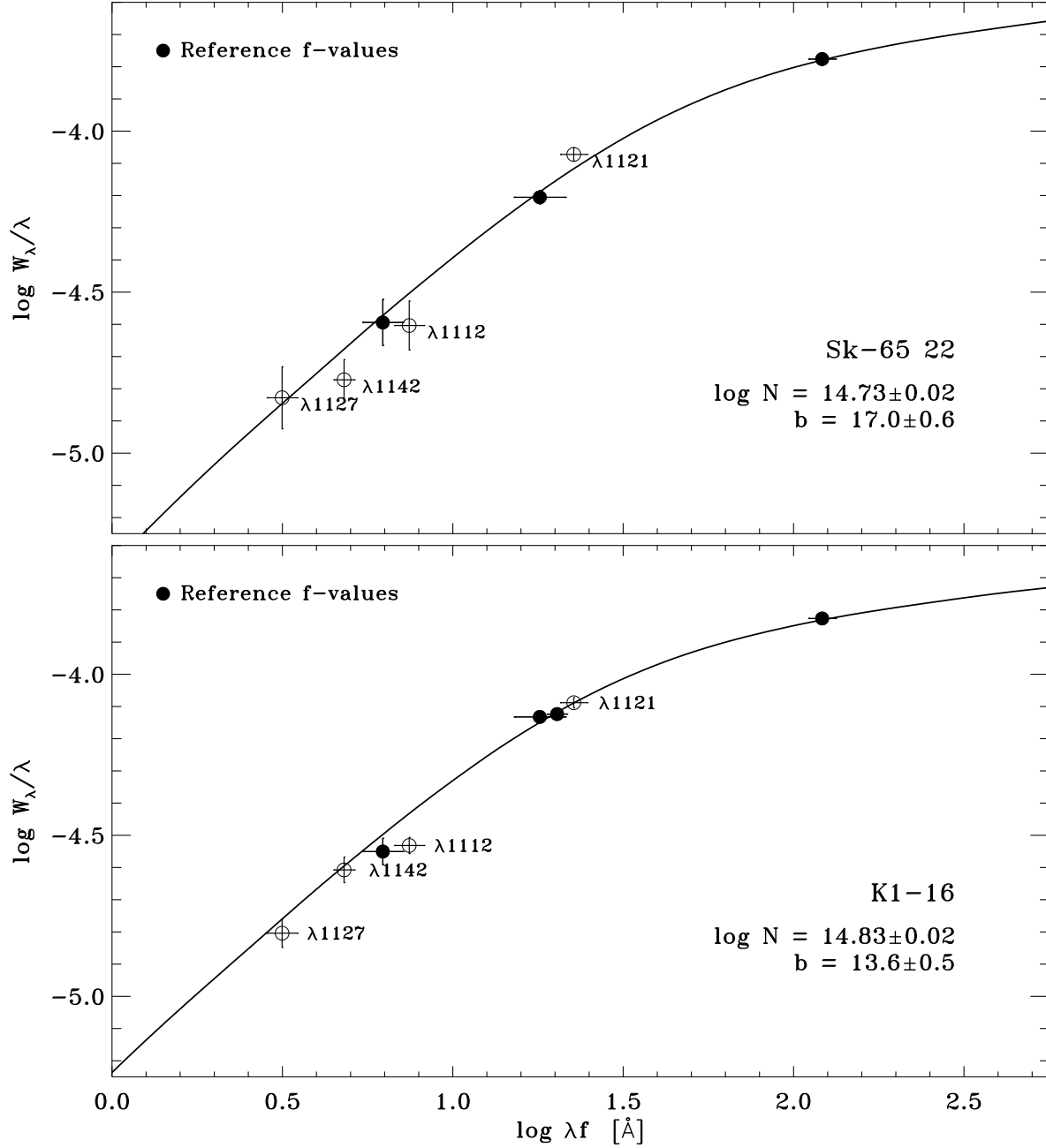


Fig. 8.— The best-fit, single-component curves of growth for the Sk-65 22 (*top*) and K1-16 (*bottom*) Fe II data. The curves were fit to the $\lambda\lambda 1125$, 1133, 1143, and 1144 equivalent widths (plotted as filled circles), where measured, using RU98 the oscillator strengths. The open circles denote FUV transitions for which we have used the curves of growth to calculate the f -values. These transitions, at 1112, 1121, 1127, and 1142 Å, are placed on the plots using our final oscillator strength estimates (see Table 1). The column densities and b -values derived from these curves of growth are shown for each sightline. Towards Sk-65 22 these data sample only Milky Way material.

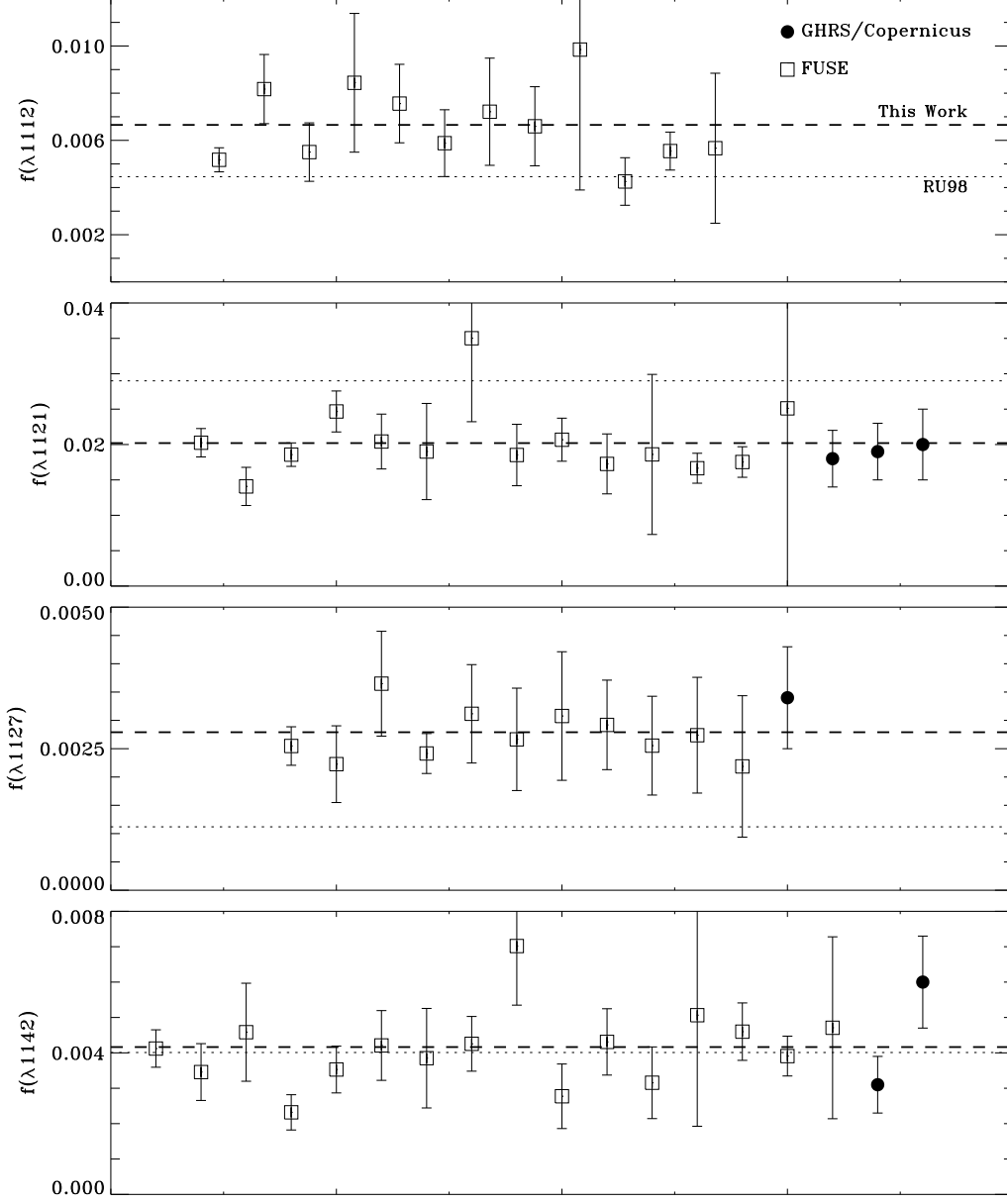


Fig. 9.— Distribution of the individual measurements f_{λ}^i of the oscillator strengths of $\lambda\lambda 1112.048$, 1121.975 , 1127.098 , and 1142.366 . The open squares represent estimates derived from *FUSE* data, while the filled circles denote estimates derived from *GHR* and/or *Copernicus* data. The dotted lines show the oscillator strengths calculated by RU98, while the thick dashed lines show the final average values derived in this work.

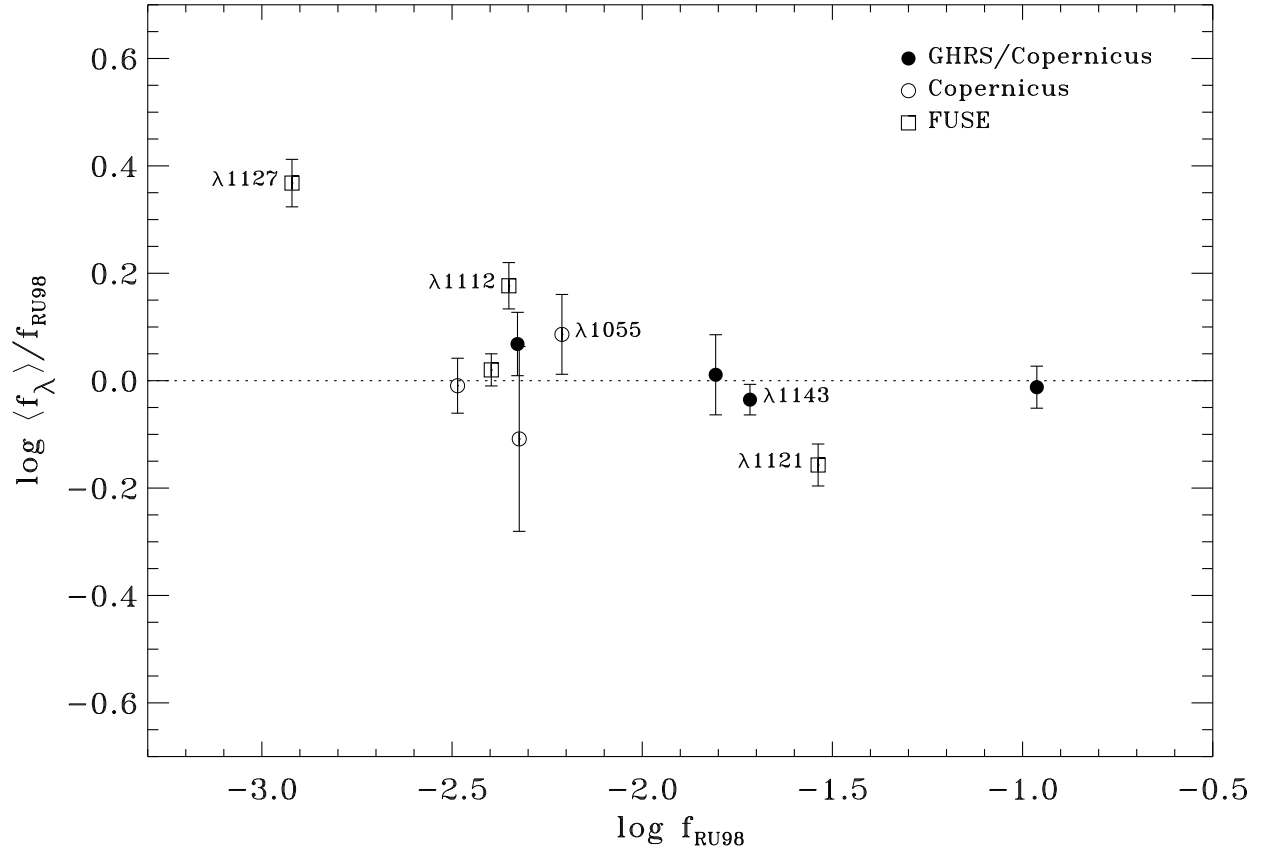


Fig. 10.— The ratio of the final average oscillator strengths derived in this work (see Table 1) to those calculated by RU98 versus the RU98 strengths. Filled circles denote measurements that rely on *Copernicus* and/or GHRs data; the open circles are based only upon *Copernicus* data; and the open squares indicate estimates that include data from *FUSE*. In general the agreement between our best empirically-derived f -values and those calculated by RU98. Important exceptions include the lines at 1112.048, 1121.975, and 1127.098 Å.